ICAS Paper No. 68-02

RESULTS OF RECENT NASA RESEARCH PERTINENT TO AIRCRAFT NOISE AND SONIC BOOM ALLEVIATION

by

Harvey H. Hubbard, Acoustics Branch,

Domenic J. Maglieri, Aircraft Noise Control Section,

and

William H. Mayes

NASA-Langley Research Center
Hampton, Virginia, U.S.A.

The Sixth Congress of the International Council of the Aeronautical Sciences

DEUTSCHES MUSEUM, MÜNCHEN, GERMANY/SEPTEMBER 9-13, 1968

Preis: DM 2.00

RESULTS OF RECENT NASA RESEARCH PERTINENT TO AIRCRAFT NOISE AND SONIC-BOOM ALLEVIATION

Harvey H. Hubbard, Domenic J. Maglieri, and William H. Mayes
NASA Langley Research Center
Langley Station, Hampton, Va.

INTRODUCTION

This paper deals with the airport-community noise problem associated with landing and take-off operations and with certain aspects of the sonic-boom problem associated with high-speed flight. The material is derived from portions of a broad acoustics research program dealing with various aspects of the above problems. Figure 1 illustrates the general nature of these problems and indicates some specific topics to be covered.

Noise in communities surrounding airports is largely due to the power plants, and sizable areas adjacent to the airports are exposed to this noise during aircraft operations (see refs. 1 to 4). The general nature of these exposed areas is illustrated by the plan-view sketches on the left side of Figure 1. During landing approach a relatively small area is exposed to rather high noise levels. On the other hand during the take-off climbout operation, much larger areas are exposed to relatively lower noise levels.

In the case of supersonic aircraft, noise due to shock-wave impingement on the ground will be experienced during the major part of the supersonic phase of the flight. As indicated by the sketch on the right, shock-wave noise is first observed during the transition phase of the operation, and exposure patterns get wider and the intensities lower during the high-altitude cruise. It should be noted that the area exposed to shock-wave noise can be 50 miles wide and thousands of miles long, and thus is significantly larger than those areas routinely exposed to engine noise.

With regard to the engines, research is aimed at reducing noise in the engine and its components, absorbing noise in the nacelle ducts before it radiates into free space, and operating the aircraft to minimize the ground-noise exposures.

With regard to shock-wave noise, consideration is given to the generation of the shock waves as influenced by aircraft design, the propagation of the shock waves through the atmosphere, and the associated variability observed as a result of atmospheric effects (see refs. 5 to 8). The significance of various aircraft operational factors such as altitude, Mach number, and acceleration are discussed. Some attention is given to the developing technology in the area of simulation of sonic-boom signatures in special studies relating to the effects on structures, people, animals, and so forth. Finally, a brief discussion regarding the results of recent studies relating to the effects problem is presented.

ENGINE NOISE REDUCTION

Engine Cycle Considerations

One of the main objectives of research on exhaust noise reduction is to find acceptable methods of producing less noise per unit thrust. The fan or bypass engine offers the possibility for lower exhaust velocities and hence lower exhaust noise levels. The data of Figure 2 are included to show the relative perceived noise levels associated with various engine types (ref. 3). Maximum perceived noise levels at a sideline distance of 200 feet were estimated and were arbitrarily normalized to a thrust of 21,000 pounds. They have been plotted as a function of bypass flow ratio, referred to those of the turbojet engine.

Data for current turbojets are plotted at the zero location of the abscissa scale and fall in the narrow hatched region. Current turbofans are represented by the larger hatched region and are seen to have somewhat lower perceived noise levels. Proposed high bypass ratio engines are represented by the stippled region at the right, and it is seen that by means of an increase in bypass flow ratio, substantially lower perceived noise levels may be realized. The lower boundary of the stippled region is well defined by the jet exhaust noise, but the upper boundary is not well defined. The vertical extent of the stippled region represents some of the uncertainities regarding compressor, fan, and turbine noise for these proposed engines and indicates the possible gains to be achieved by specialized noise-reduction procedures. Research effort is being directed to minimize the noise from the above sources so that the full noise-reduction potential of these engines can be realized.

Noise Due to Aerodynamic Interactions

The fan and compressor sections of current fan engines are important sources of noise. Since the trend in commercial aircraft engines is toward higher bypass flow ratios, it follows that noise from the rotating components of these future engines may be relatively more intense. Considerable effort has been directed toward studies of the noise generation by compressors and fans and in ways of reducing this noise. One of the ways in which such noise can be reduced at the source is by including the proper spacing between stationary and rotating components of the engine.

Figure 3 contains schematic diagrams which illustrate some of the main features of the aerodynamic wakes of the stationary vanes and the resulting load fluctuations on the rotor due to such wakes (ref. 3). There is a velocity deficiency in the wake as indicated by the dark shaded regions. The velocity deficiency is strongest near the stationary vane where the wake is narrowest. As the wake broadens out at greater distances, the velocity deficiency decreases. Thus, a rotor blade passing through the wake of the stationary vane will encounter different flow

conditions depending on the portion of the wake that it encounters. As the rotor blade passes through the wake, it experiences a momentary change in angle of attack due to the variation in in-flow velocity, and thus there is an associated fluctuation in the blade loading. The sketches at the bottom of the figure are artist's conceptions of these load increments as a function of spacing between the stationary vane and the rotor. It is believed that the blade-load fluctuations are of shortest duration and of greatest magnitude when the clearance between the two is relatively small. As the clearance increases, the amplitudes are reduced and the durations increase. Since it is believed that the noise from the rotating components is directly related to the blade-load fluctuations, there is a suggestion that an increased spacing is beneficial with regard to noise reduction.

The existence of pure tone components in engine-noise spectra has been recognized as being generally detrimental to community acceptance, and several studies have been conducted to evaluate the subjective effects of the presence of such pure tones. An example of some of the recent results is illustrated by the spectra of Figure 4.

The solid curve represents a broad band background noise on which is superposed a pure tone component (ref. 9). The pure tone amplitude is about 10 dB higher than the level of the background noise in the corresponding frequency band. For such a situation, the subjective evaluations obtained by paired-comparison procedures indicate the noisiness to be equivalent to that represented by the dashed curve spectrum. The presence of the pure tone would produce the same noisiness as an across-the-board increase of about 6 dB in all frequency bands. The reduction of the levels of pure tones is a main objective of the following noise-alleviation methods.

Inlet Flow Choking

One method of inlet flow choking involves modifications to the inlet guide vanes in such a way that higher than normal Mach number inlet flows exist in the guide vane row. Studies of this phenomenon have been made on a research compressor in an anechoic room and the main findings are shown in Figures 5 to 7 (ref. 10). Shown in Figure 5 are the overall sound-pressure levels observed in front of the compressor as a function of Mach number in the inlet guide vanes. For a given inlet guide-vane configuration, Mach number was increased by increasing the speed of the rotor. For the particular configuration of the figure, maximum noise levels were observed at a Mach number in the guide vane of about 0.65 and noise reductions occurred at higher Mach numbers. At Mach numbers in the near vicinity of 1.0 there is a dramatic decrease in noise level due to aerodynamic choking.

The data of Figure 6 indicate the ranges of noise reduction observed for various rotational speeds and inlet guide-vane configurations. Shown at the top of the figure is a hatched region representing the noise reductions obtained by increasing the spacing between the inlet guide vanes and first-stage rotor in order to reduce the aerodynamic interactions. The bottom boundary of this region represents the case where inlet guide vanes were removed completely or were operating so as to essentially eliminate the aerodynamic interactions which are the main noise sources. The shaded region to the far right indicates the additional noise reduction obtained by means of flow choking in the inlet guide vanes. In order to widen the speed range over which inlet guide vane choking could be accomplished, the vanes were both thickened and turned through an angle. By this means, flow choking was accomplished at rotational speeds lower than 100 percent. These dramatic results suggest that variable geometry inlet guide vanes would be useful from a noise-reduction standpoint.

As a result of experience with both laboratory devices and actual engines (ref. 11), the potential noise reductions associated with various inlet guide-vane configuration variables are summarized in Figure 7. The relative inlet noise levels are shown on the vertical scale for various inlet guide-vane configurations for both the take-off-climbout and landing-approach situations. Complete removal of the inlet guide vanes has been accomplished in some recent advanced engine designs to eliminate the first-stage aerodynamic interactions. Inlet choking by means of variable-geometry guide vanes would produce sizable noise reductions but at the expense of added mechanical complexity. The concept of using increased inlet guide-vane clearance while at the same time retaining the ability to choke the inlet flow by means of variable-geometry guide vanes may be highly desirable. If the choke feature were not needed, some modest noise reduction would accrue naturally because of the decreased aerodynamic interactions. The operator could conceivably elect to use the choke feature only if it were needed for particular situations. Such an approach to design would give the operator of the aircraft desirable flexibility with regard to noise exposures and thus would seem to be a very attractive development for future engines.

Nacelle Acoustic Treatment

One very attractive development, not only for future fan engines but also as a possibility for retrofit modifications to current engines, is the incorporation of sound-absorbing material in the inlet and fan discharge ducts (ref. 12). Examples of the application of such techniques are given in Figures 8 and 9. Figure 8 shows photographs of some model inlets and the associated schematic diagram indicating the surface areas in the inlet to which special sound absorption treatments are applied. The configuration on the left is referred to as the concentric ring inlet and has a multiple ring splitter oriented generally parallel to the flow in the space between the center body and the cowl surface. The configuration on the right is referred to as the "litebulb" configuration. Its distinguishing feature is an enlarged bulbous center body. The concept, represented by the enlarged center body, is to minimize the "line of sight" noise propagation from the face of the compressor or fan. The acoustic performance of these two configurations is comparable, but the concentric ring inlet is more attractive because of aerodynamic considerations.

Combinations of treated inlets and treated fan discharge ducts are illustrated schematically in Figure 9. The top sketch represents a configuration using a so-called short duct treatment for the

fan discharge, and the bottom sketch represents a long duct treatment. These two fan duct configurations in conjunction with the appropriate treated inlets are designed to produce different amounts of overall flyover noise reduction. The top configuration is estimated to produce 7 to 10 PNdB noise reduction and the bottom configuration approximately 12 to 15 PNdB. They represent passive treatments and no variable geometry is involved. Such configurations as those illustrated in Figure 10 would provide the operator with some flexibility regarding operational noise-reduction requirements.

The reason for treating both the inlet and the fan discharge ducts acoustically to reduce flyover noise is evident from the data of Figure 10. It can be seen that two noise peaks exist, and these are associated with noise from the inlet and the fan discharge ducts, respectively. The data of the bar graph are estimates of the perceived noise-level reduction that might be obtained during the landing-approach operation by treating portions of the engine nacelles. Acoustic treatment of the inlets only would probably not reduce the maximum noise levels but would essentially eliminate the first peak of the noise time history. The resulting perceived noise-level reduction would be a modest one. Likewise, if the discharge ducts alone were treated, this would essentially eliminate the second peak in the noise time history and a somewhat larger but still modest perceived noise-level reduction would result. If, however, the inlet and the fan discharge ducts were both treated, a rather substantial overall noise reduction would be estimated as shown by the bar at the bottom.

Aircraft Operations

Noise during take-off-climbout operations of commercial aircraft is an important consideration because of possible adverse reactions in communities near airports. Data have been collected under controlled conditions for several jet transport aircraft to determine operating procedures during climbout which will minimize noise exposures.

The data of Figure 11 illustrate the perceived noise-level reductions obtainable by power cutbacks for aircraft having different types of jet power plants (ref. 13). The sketch at the upper left relates to a four-engine turbojet-powered aircraft. It can be seen that the reduction in perceived noise level at the time of the power cutback is of the order of 10 PNdB. In the sketch at the lower left, similar data for a four-engine turbofan-powered aircraft indicate a smaller noise-level reduction. The lesser reduction obtainable for the turbofan is due to the presence of fan noise. The sketches at the lower right relate to two- and three-engine fan-powered aircraft, and it is seen here that the perceived noise-level reductions due to power cutback are relatively larger. Portions of such reductions result from special design features of these particular turbofans to reduce fan noise. The amount of noise reduction obtained through power cutback is a function of the type of aircraft as well as the type of power plant and its detailed design features, and hence no generalizations can be made.

Aircraft-Noise-Certification

The possibility of certifying new aircraft with respect to their noise characteristics has focused attention on several associated technical problems. Such an item as the definition of a noise-evaluation unit is an obvious requirement. The statistical variability both of noise measurements and of noise predictions due to weather, terrain effects, and operating procedures is of particular concern. Finally, the problem of making adequate noise-evaluation measurements, particularly for very large heavy aircraft, is a difficult problem. Some consideration has been given to possible procedures for accomplishing this latter task, and Figures 12 and 13 present some preliminary results.

The noise exposures at ground level from the climbout operation of a particular aircraft are a function of several factors such as the aircraft speed, weight, climb rate and altitude, flap setting, and engine thrust level. These are not independent variables but rather are interrelated. A procedure has been devised which involves controlled flight-noise measurements to properly account for the effects of all of these factors and which may eliminate the need for actual take-offs and landings during noise evaluation tests. The nature of this procedure is illustrated in Figure 12 (ref. 13). The aircraft, under radar control, was flown in a level flight attitude to the vicinity of the acoustic range. Just prior to reaching the acoustic range, the engine throttle settings were adjusted to provide various rates of climb from 750 to 2,400 feet per minute. Data were recorded at each noise-measuring station as the aircraft passed overhead. Tests were repeated for each of several initial flight altitudes and climb rates. By these means acoustic data were obtained for appropriate combinations of aircraft altitude, speed, engine thrust setting, and flap setting.

The usefulness of such parametric data for predicting the noise for a given climbout profile has been evaluated and preliminary results are illustrated in Figure 13. This profile defined by the solid line at the top involved take-off power with 14° flaps to 1500 feet altitude with subsequent power reductions to produce a climb rate of 500 fpm. Deviations from the planned profile for three runs are represented by the hatched areas. Perceived noise-level data are plotted as a function of distance from start of roll at the bottom of the figure. For comparison, estimates have been made for the associated perceived noise levels based on the parametric flight studies described above for the appropriate thrust and altitudes of the given profile, and these estimates are represented by the two solid curves in the bottom sketch. It can be seen that fairly good correlation exists between the measured perceived noise levels and those estimated from the parametric studies.

The use of the parametric flight concept for the ground-noise evaluation of an aircraft in flight may be particularly useful because it eliminates the need for repeated take-offs and landings. Aircraft weight does not have to be duplicated nor is it necessary to make the measurements at an airport. In order to fully exploit this method, the aircraft has to be under positive control at all times, and thus the instrument requirements for tracking and for acoustic measurements are the same as for other methods.

SHOCK-WAVE NOISE

Shock-wave noise is a factor only for supersonic flight and thus is of concern during the transition and cruise phases of the mission. It is associated with the shock waves from the aircraft and is observed as explosive sounds or booms that usually occur without warning. Because of its ability to shake buildings and to cause annoyance, it poses a unique problem for the orderly development of high-speed air transportation. As a result, considerable research has been performed regarding various aspects of the problem. Sample results relating to studies of generation and propagation phenomena, operational factors, laboratory simulation, and effects are included herein.

Design Considerations

Analytical procedures are available for describing the entire flow field of a body in supersonic flight (ref. 5). These methods, which make use of machine computing procedures, have made it possible to study means of minimizing the sonic boom by variations in design. Some of these minimization concepts are illustrated in Figure 14. Use is made of the equivalent body concept in the presentation of the data. The equivalent cross-sectional areas as a function of axial distance are shown schematically at the top for three different designs, and the relative contributions of the volume and lift components are indicated.

The relatively blunt design at the left has been found to yield the minimum overpressure at all distances. Because of the high shock losses, the drag is high and the shape is not considered practical for aircraft.

The area development in the middle yields a minimum or near minimum of positive overpressures in the near-field and mid-field. This results in a flat-topped signature. The corresponding aircraft shape suggested by this minimization approach appears to be practical since proposed designs are long and slender enough for the mid-field effects to persist to the ground, and drag penalties do not necessarily result.

For larger airplanes, the shape shown at the right might be considered for the purpose of generating a finite rise time wave. There is some question about the practical application of this principle, however, because of the extreme airplane length required.

The illustrations of Figure 14 relate directly to the bow wave of the signature. Similar modifications to the rear portion of the airplane would have to be considered for tail wave effects.

The analytical procedures used in the studies of Figure 14 have been validated in wind-tunnel experiments for which atmospheric variability was not involved.

Signature Variability

An indication of the measured variations in wave shapes at ground level is given in Figure 15 for airplanes of three different sizes (ref. 8). The associated durations are approximately 0.1, 0.2, and 0.3 sec. These signatures fall into three general classes: normal signatures closely resembling theoretically calculated N-waves, peak signatures wherein the peak pressure is enhanced relative to the basic N-wave, and rounded signatures with longer rise times and lower peaks than the N-wave. Combinations and variations of these signatures also occur. The main differences between waves for different aircraft occur at the time of the rapid compressions. The largest overpressure values are generally associated with sharply peaked waves.

In one of the recent studies with the F-104 airplane, an 8000-foot horizontal (2.44 km) range instrumented with about 40 microphones was employed for atmospheric effects studies. Figure 16 shows some results for the overpressures, which indicate a wavelike pattern. Experimental results suggest that this is a moving pattern and that there is a gradual change from peaked to rounded signature shapes. Measured positive impulses also show a wavelike pattern, but their variability is considerably reduced.

Shown in Figure 17 are the calculated amplitude-squared, or energy spectra of two signatures having different shapes. Only relatively small changes occur in the envelopes of the amplitudes, despite the differences in shape. Calculations of the relative phases showed that the lower frequencies of the spectra appear well correlated and coherent, whereas for the higher frequencies the relative phases of the two waves tend to become random. It is thus suggested that the effects of the atmosphere may lead to a phase-scrambling process for the higher frequencies (ref. 8).

Probability Distributions

In some cases where a sufficient number of data points are available, probability distributions have been prepared. Examples of this type of data are shown in Figure 18 as the probability of equaling or exceeding certain values of the ratio of measured-to-calculated nominal overpressures. Also included are histograms of the pressure amplitudes. The data of the 8,000-foot-long microphone array for a Mach number of 1.3 are represented by the circle data points and the data for the higher Mach number by the diamond data points (ref. 14). It can be seen that the data generally fall on straight lines with the exception of a few points at the extremities, and thus they follow generally a log normal distribution. It can be seen that different variability exists between the two sets of data as suggested by the slopes of the curves. Lesser variability in the overpressure was observed for the higher Mach number data for which the ray paths were shorter and more nearly vertical.

In conjunction with some XB-70 flights, a number of accompanying flights of B-58 and F-104 airplanes were made (ref. 8). The Mach number and altitude ranges covered were from $M = 1.5$ to 2.5 and $h = 11.3$ to about 18 km, respectively, for the XB-70 airplane; $M = 1.5$ to 1.65 and $h = 9.7$ to 12.2 km, respectively, for the B-58 airplane; and $M = 1.3$ to 1.4 and $h = 5.2$ to 6.3 km, respectively, for the F-104 airplane. The nominal calculated over-pressure for all these airplanes was about 2 pounds per square foot. The data in Figure 19 for the three airplanes were obtained in late morning flights from November 1966 to January 1967, when convective activity and associated

turbulence were light. Despite the differences in airplane operating conditions and signature durations, a strikingly similar probability distribution pattern for the three airplanes appears.

Aircraft Operational Factors

A series of ground-pressure measurements has been made for longitudinal aircraft accelerations from Mach 0.9 to about Mach 1.5 at a constant altitude of 37,200 feet with a special array of microphones extending about 23 miles along the ground track. The measured data points from three such acceleration flights are shown at the bottom of Figure 20. The data at the zero position represent the so-called superboom condition where pressure buildups occur (ref. 15). The data for three separate flights were normalized by plotting the highest measured overpressure values at this zero position. The direction of the aircraft is from left to right, as indicated by the sketches at the top, along with corresponding tracings of measured signatures. The data points in the figure represent peak overpressures as defined in the sketch. The low-value points to the left of the figure represent noise and are observed as rumbles. The high-value points near the center of the figure correspond to measurements that are very close to the focus point, and thus represent what are conventionally described as superbooms. To the right of the focus point are two distinct sets of measurements which relate to the region of multiple booms. For convenience in illustrating the trends of the data, solid and dashed lines are faired through the data points. The data points that cluster about the solid curve relate to the first signature to arrive, in all cases, and this eventually develops into the steady-state signature. The data points that cluster about the dashed curve relate, in all cases, to the second signature to arrive. These values generally decrease as distance increases, and eventually this second wave ceases to exist because of the refraction effects of the atmosphere.

The highest overpressures are measured in a very localized region. These values are as high as 2.5 times the maximum value observed in the multiple-boom region and are thus in general agreement with the measured results for lower altitude tests. The main multiple-boom overpressure values are of the same order of magnitude as those predicted for comparable steady-state flight conditions. Available overpressure prediction methods give good agreement in the multiple-boom region but are not considered reliable in the superboom region.

The locations of the superboom and multiple-boom regions are readily predictable provided such information as flight path, altitude, and acceleration rate of the aircraft is available. Based on the experience presented in Figure 20, it is believed that the superboom can be placed at a position on the ground to within about ±5 miles of the desired location. The prediction of the location of the superboom can be improved if more detailed weather information is available.

Sonic-Boom Simulation

Because of the complexity and high cost of studying the effects of sonic booms by means of aircraft flyovers, there is strong motivation to develop means of simulating sonic-boom signatures for laboratory purposes. Various approaches to simulation have been pursued, and various devices have evolved. None of these devices to date are capable of the generation of arbitrary signatures under controlled conditions; however, the simulations have been very useful for some specialized purposes. Examples are shown in Figures 21 to 23.

The exposure of the whole body to sudden N-wave type pressure changes resembling outside boom exposures has been accomplished by the small cubicle of Figure 21(a) (see ref. 16). Exposure of a person, plus the structure by which he is protected, has been accomplished by the multiple chamber arrangement of Figure 21(b), which accomplishes the generation of room vibrations as well as the acoustic stimuli (ref. 17).

A device involving the generation of traveling shock waves is shown in the photograph of Figure 22. This was developed initially for microphone calibrations where an impinging shock wave was desired. A further development of the calibration device included a large horn and accessories to produce multiple shocklike disturbances in the open air (ref. 18). These disturbances simulate the high-frequency portion of the signature but do not properly simulate the low-frequency portion. The device, as shown in the photograph, has been used in behavioral studies of domestic animals.

The explosive charge simulators pictured schematically in Figure 23 were developed for outdoor use and for the exposure of large objects such as a whole building structure. The folded line charge configuration generates an N-wave type disturbance, but it is of relatively short duration. The "stacked" configuration generates a relatively longer N-wave type pressure signature. Both of these approaches result in pressure signatures which have an unacceptable amount of high-frequency hash which may be associated with rough burning of the explosives. The bottom configuration which involves a gasbag envelope was conceived as a possible means of smoothing the burning and thus eliminating the unwanted high frequencies. This last configuration has not been fully evaluated.

Sonic-Boom Effects

The sketch at the top of Figure 24 illustrates the outside and inside exposure situations for people (ref. 5). In the inside exposure case, the building acts as a filter which determines the nature of the exposure stimuli reaching the observer. The ingredients of the inside exposure situation are included in the chain diagram at the bottom of the figure. The sonic-boom-induced excitation of the building which causes it to vibrate may arrive either through the air or through the ground and can be observed directly by the subject. The building vibrations may also generate observable noise or, in the extreme case, may lead to minor damage.

Seismic Responses

A systematic study of sonic-boom-induced seismic responses was conducted, involving flights of a large number of airplanes and analytical studies (ref. 19). The nature of the ground-motion problem is suggested by the data of Figure 25. At the left of the figure is a sketch of the pressure front on the ground from an aircraft in flight (solid curve). The dashed curves represent the associated seismic fronts as they might appear at

some later time. Provided the seismic disturbances could propagate over appreciable distances, there might be a focal point on or near the track. To date there is no direct experimental evidence of such focusing.

A representative seismogram is shown on the right-hand side of the figure. The solid line is a measured ground particle-velocity signature, and the dashed line represents a particle-velocity calculation by a simple theory which assumes a traveling airload over an elastic medium. It can be seen that the theory seems to account for the maximum particle-velocity values, and hence the traveling load effect is judged to be the dominant one. Other features of the ground-response signature are identifiable. For instance, the lower frequency oscillations are associated with Rayleigh waves, the frequency of which varies as the speed of the airplane varies. The higher frequency is related to reflections from a subsurface layer and hence is a function of the local geology.

The measured particle velocities for several different types of aircraft as a function of sonic-boom overpressure are shown by the shaded region in Figure 26. There seems to be a roughly linear relationship between particle velocity and sonic-boom overpressure. The maximum particle-velocity readings are about 100 microns per second for each 1 pound per square foot of overpressure. The highest values recorded during the experiments are about 1 percent of those measured for earthquakes which just begin to cause observable damage.

Building Response

In Figure 27 is an N-type pressure signature that, for proposed supersonic transports in cruise flight, may be of the order of 300 meters in length (ref. 5). The sketches at the bottom of the figure suggest that a building is subjected to a variety of loading events as the wave pattern sweeps over it. For instance, reading from left to right, the building first would be forced laterally as a result of the initial positive loading on the front surface. Then it would be forced inward from all directions, then forced outward, and finally forced laterally again because of negative pressures acting on the back surface. This loading sequence, which would be applied within a time period of about 0.3 second, can result in complex transient vibrations of the building.

The loading patterns of Figure 27 relate to the situation in which the building is sealed to prevent venting of pressures from outside to inside. In such cases, air-cavity structural coupling is important in determining vibration responses of carpentered structures (ref. 5). The data of Figure 28 represent sample results for the case of a room with a partly opened window being excited during an aircraft flyover. The outside pressure trace is indicated at the top. The inside pressure trace with the window closed is given in the middle. The bottom trace represents the condition for the window partly opened in such a way as to create a Helmholtz resonator. It can be seen that the pressure fluctuation for the resonator case can be higher in amplitude than the exciting pressure. It has the appearance of a damped sine wave, and persists for a longer period of time than the initial excitation wave.

The data of Figures 29 and 30 apply to the forced vibration of house-type structures from the unpublished work of Findley, Carden, and Dibble and indicate the nature of their vibration response. The solid curve of Figure 29 represents the relative acceleration levels as a function of frequency for a given input force level. It can be seen that the acceleration responses generally increase with frequency over the range of the tests. The peaks of this response curve are associated with particular modal responses of the house. The upper sketch indicates a response mode involving the walls of a room at a relatively low driving frequency. The main feature of such "box" responses is the conservation of volume, that is, when some walls are deflecting inward, others are deflecting outward.

The two sketches at the right represent the modal responses of one of the walls. Although these modal patterns are more complex, as the frequency increases, the conservation of volume concept still applies. The low-frequency vibration modes are generally associated with the beams, rafters, joists, and so forth, whereas the high frequencies are associated with the wall panels.

From a subjective standpoint, the motions of the walls of the house may be important both because of the associated noise and the observed vibrations. One source of noise is the vibration of hanging objects attached to the walls. Such a case is illustrated in the data of Figure 30. Wall accelerations with and without a mirror are presented as a function of force input to an adjacent wall. The acceleration increases directly as the force increases for the wall alone in the range of the tests. With the mirror attached, a vibration level can be reached at which the mirror can no longer follow the motions of the wall. At this condition the mirror impacts the wall in an erratic manner and rattling is observed. Such rattling, which is easily curable, is known to be important subjectively.

Subjective Reactions

The manner in which people react to sonic booms is dependent to some extent upon whether they are located indoors or outdoors. A person indoors, as indicated in Figure 24, may observe directly the vibration of a building and the associated noise radiation. Results of tests to compare the subjective reactions of people to indoor and outdoor boom exposures have suggested that the above building-response phenomena were detrimental and the indoor booms were thus rated slightly less acceptable.

For the outdoor situation, the loudness of the booms and the associated startle effects are significant and these depend upon the peak overpressure and the rate of onset of overpressure (rise time). Results of subjective tests of people in a sonic-boom simulator in which rise time was varied are presented in Figure 31 (ref. 16). Relative annoyance level is shown as a function of rise time. The stippled region represents observations from a number of subjects and for a range of signature durations. It can be seen that the annoyance level decreases markedly as rise time increases.

CONCLUDING REMARKS

The airport-community noise problems associated with aircraft landing- and take-off-climbout operations and with certain aspects of the sonic-boom problem associated with supersonic flight have been briefly discussed. Aircraft noise in communities surrounding airports is largely due to the power plants and improvements are indicated through the design of the engine components to generate less noise, the design of nacelles to reduce noise radiation into the atmosphere, and the operation of aircraft in take-off and landing to minimize noise exposures on the ground.

During supersonic flight the associated noise in communities is a result of the shock waves produced by the aircraft. The shock-wave noise (sonic boom) is of concern during the transition and cruise phases of the mission, because of its ability to shake buildings and cause annoyance. Research is described on various aspects of the sonic-boom problem including minimization through aircraft design and operational factors, on the development of specialized laboratory simulation devices, and on the effects on people and structures.

REFERENCES

1. Alleviation of Jet Aircraft Noise Near Airports. A report of the Jet Aircraft Noise Panel, Office of Science and Technology, Executive Office of the President, March 1966.

2. Anon.: Noise. Final report presented to Parliament by the Lord President of the Council and Minister for Science, Committee on the Problem of Noise, July 1963.

3. Hubbard, H. H.; Maglieri, D. J.; and Copeland, W. L.: Research Approaches to Alleviation of Airport Community Noise. J. Sound Vib., vol. 5, no. 2, 1967, pp. 377-390.

4. Dexter, Robert R., ed.: Proceedings of the 4th Congress of the International Council of the Aeronautical Sciences, Paris, France, August 24-28, 1964. MacMillan & Co., Ltd., 1965.

5. Seebass, A. R., ed.: Sonic Boom Research. Proceedings of a conference held at NASA, Washington, D.C., April 12, 1967. NASA SP-147.

6. Proceedings of the Sonic-Boom Symposium. J. Acous. Soc. of Amer., vol. 39, no. 5, May 1966-Part 2, pp. S1-S80.

7. Sonic-Boom Experiments at Edwards Air Force Base. An interim report prepared under Contract AF 49(638)-1758 by Stanford Research Institute for the National Sonic-Boom Evaluation Office. NSBEO-1-67. July 28, 1967.

8. Garrick, I. E.; and Maglieri, D. J.: A Summary of Results on Sonic-Boom-Pressure-Signature Variations Associated with Atmospheric Conditions. NASA TN 4588, May 1968.

9. Pearsons, Karl S.; Horonjeff, Richard D.; and Bishop, Dwight E.: Bolt Beranek and Newman, Inc., Report No. 1520 (Contract NAS1-6364), September 8, 1967.

10. Chestnutt, David: Noise Reduction by Means of Inlet-Guide-Vane Choking in an Axial-Flow Compressor. Proposed NASA TN.

11. Crigler, John L.; Copeland, W. Latham; and Morris, Garland J.: Turbojet-Engine Noise Studies to Evaluate Effects of Inlet-Guide-Vane-Rotor Spacing. Proposed NASA TN.

12. Marsh, Alan H.; Elias, I.; Hoehne, J. C.; and Frasca, R. L.: A Study of Turbofan-Engine Compressor-Noise-Suppression Techniques. NASA CR-1056, 1968.

13. Copeland, W. Latham: Noise Measurements During Take-Off-Climbout Operations of Jet Transports. Presented at the Seventy-Fourth Meeting of the Acoustical Society of America, Miami Beach, Florida, November 14-17, 1967.

14. Maglieri, Domenic J.; Huckel, Vera; Henderson, Herbert R.; and McLeod, Norman J.: Variability of Sonic-Boom Signatures Resulting From the Atmosphere as Measured Along an 8,000-Foot Linear Array. Proposed NASA TN.

15. Maglieri, Domenic J.; Hilton, David A.; and McLeod, Norman J.: Experiments on the Effects of Atmospheric Refraction and Airplane Accelerations on Sonic-Boom Ground-Pressure Patterns. NASA TN D-3520, July 1966.

16. Anon.: Human Response to Ameliorations in Specific Simulated Sonic-Boom Parameters. Lockheed-California Company Report No. LR-20922 (subcontract B-87017-US with the Stanford Research Institute), August 1967.

17. Lukas, Jerome S.; and Kryter, Karl D.: Results of Preliminary Tests of Effects of Simulated Sonic Boom on Individuals While Sleeping and Performing a Tracking Task. Prepared under Contract NAS1-6193 by Stanford Research Institute, 1968.

18. Dahlke, Hugo E.; Kantarges, George T.; Siddon, Thomas E.; and Van Houten, John J.: The Shock Expansion Tube and Its Application as a Sonic-Boom Simulator. NASA CR-1055, 1968.

19. Goforth, Tom T.; and McDonald, John A.: Seismic Effects of Sonic Booms. Geotech Report No. TR67-77 (Contract NAS1-6342), 1967.

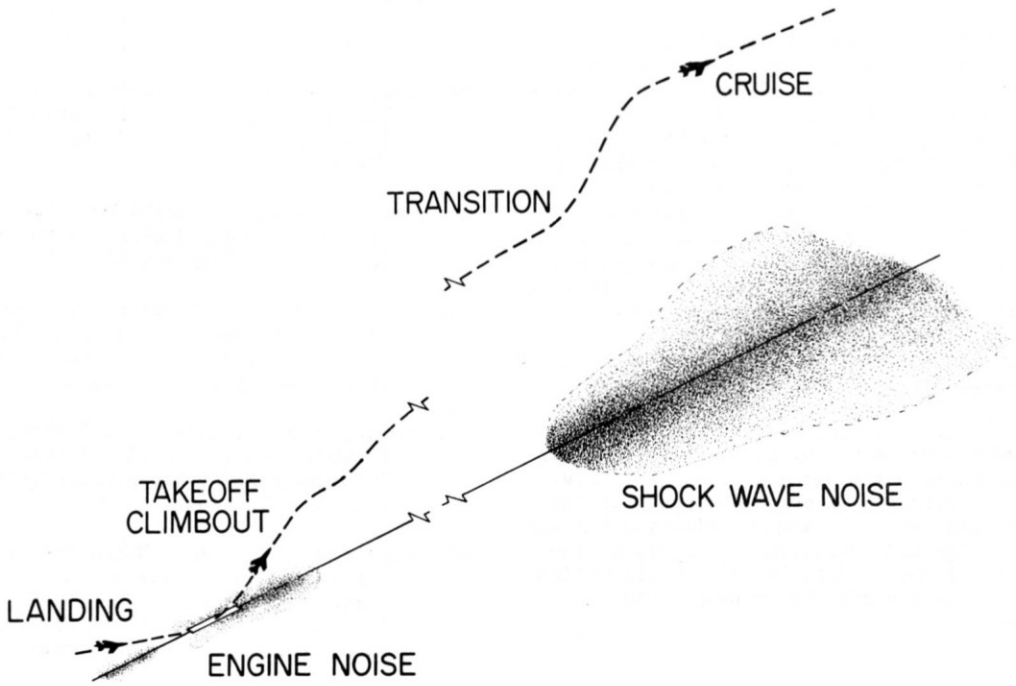

Figure 1.- Noise exposure areas.

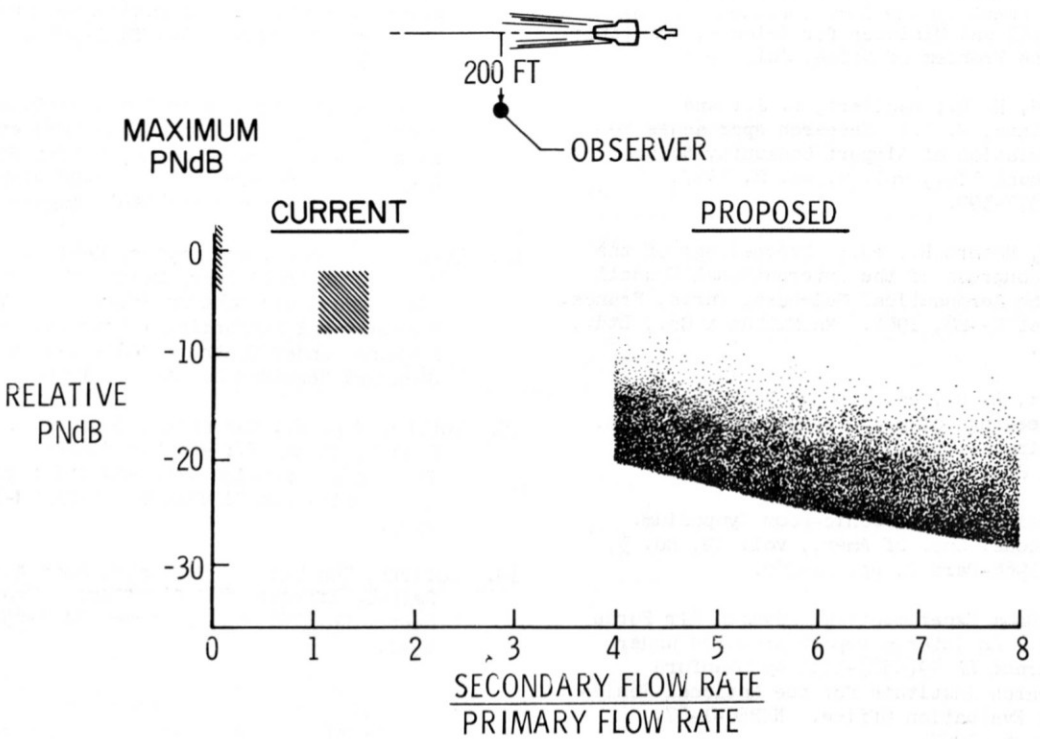

Figure 2.- Effects of engine bypass flow ratio on perceived noise level (ref. 3).

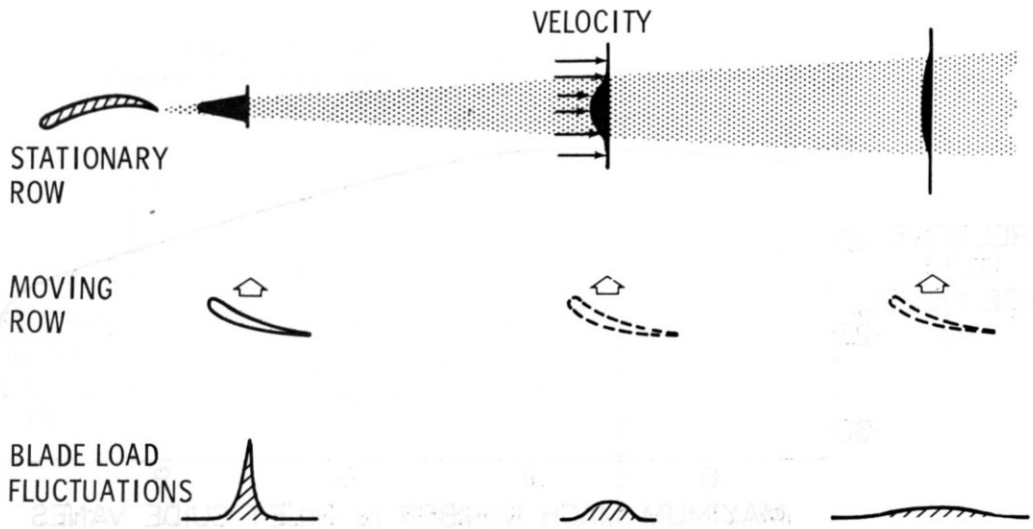

Figure 3.- Nature of inlet-guide-vane rotor interaction (ref. 3).

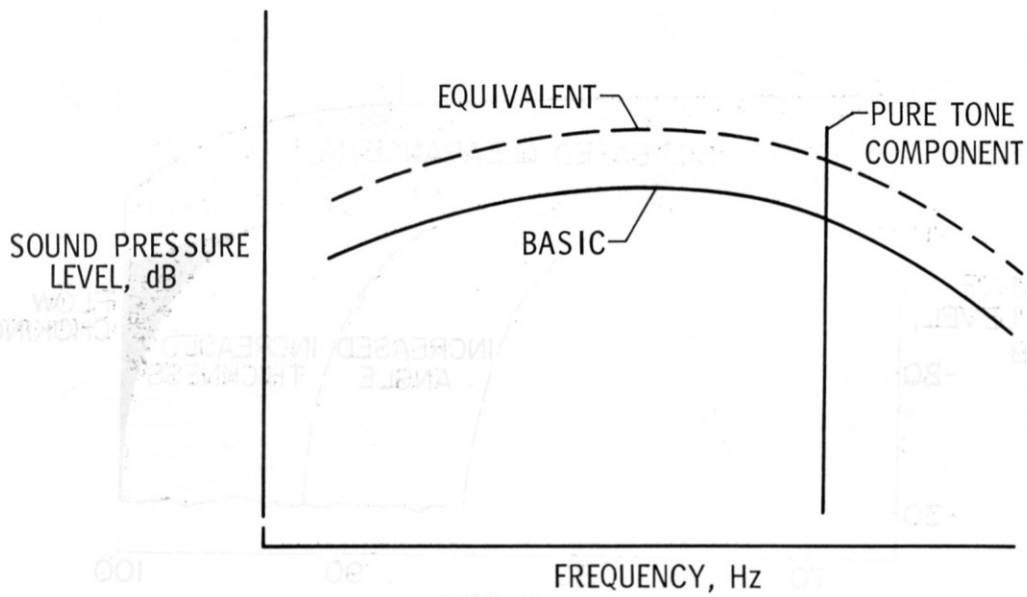

Figure 4.- Subjective effects of discrete tones (ref. 9).

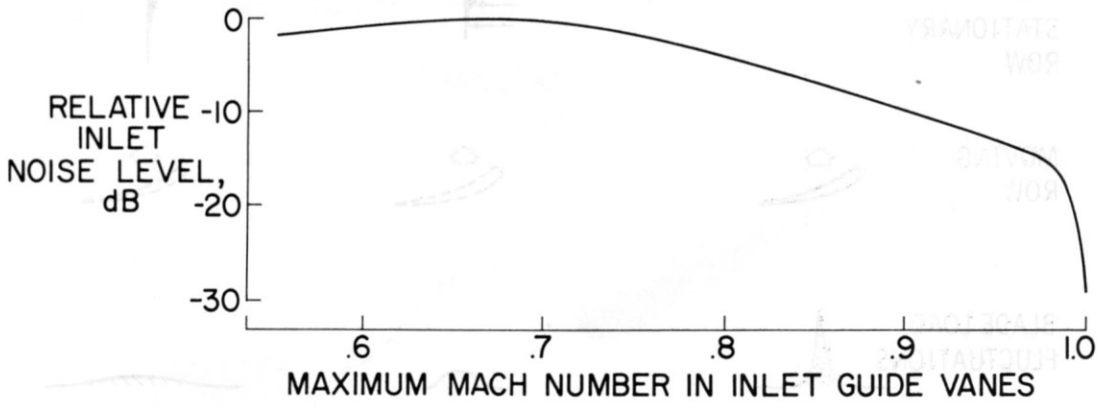

Figure 5.- Effects of Mach number in the inlet guide vanes on relative inlet noise level (ref. 10).

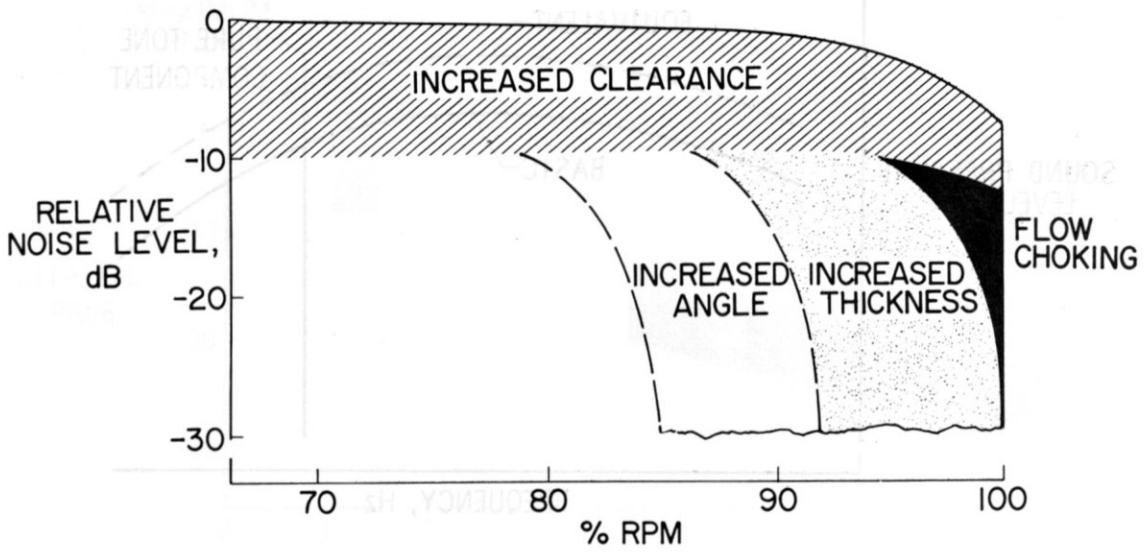

Figure 6.- Noise reductions resulting from various inlet-guide-vane configurations (ref. 10).

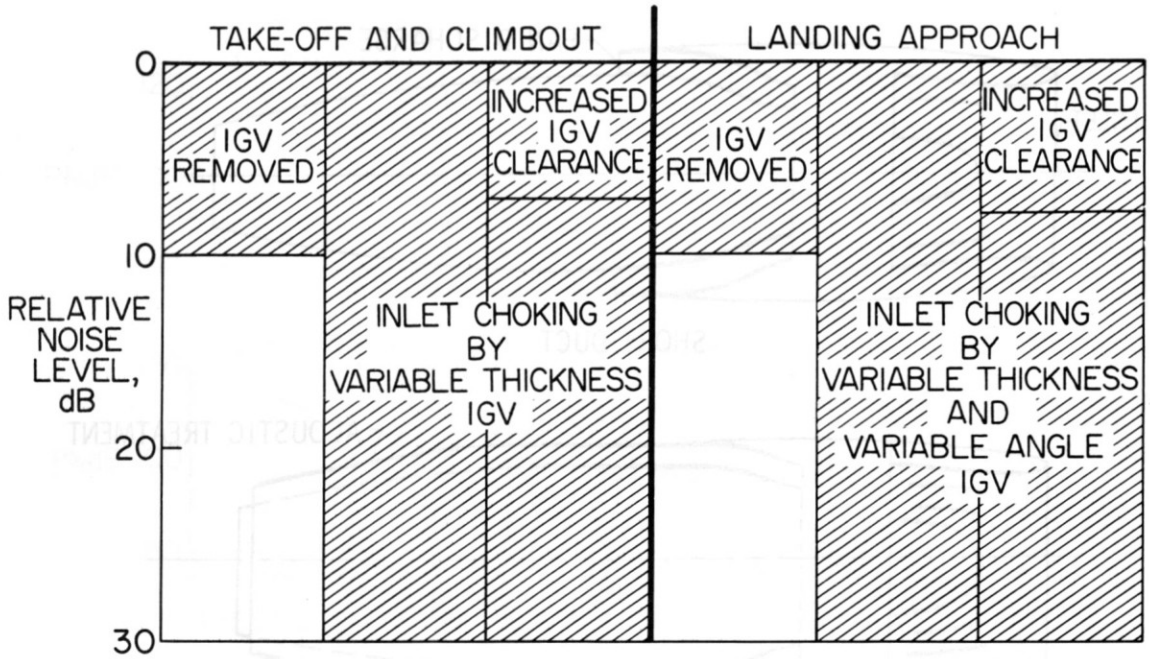

Figure 7.- Noise reduction potentials associated with inlet guide vanes (ref. 10).

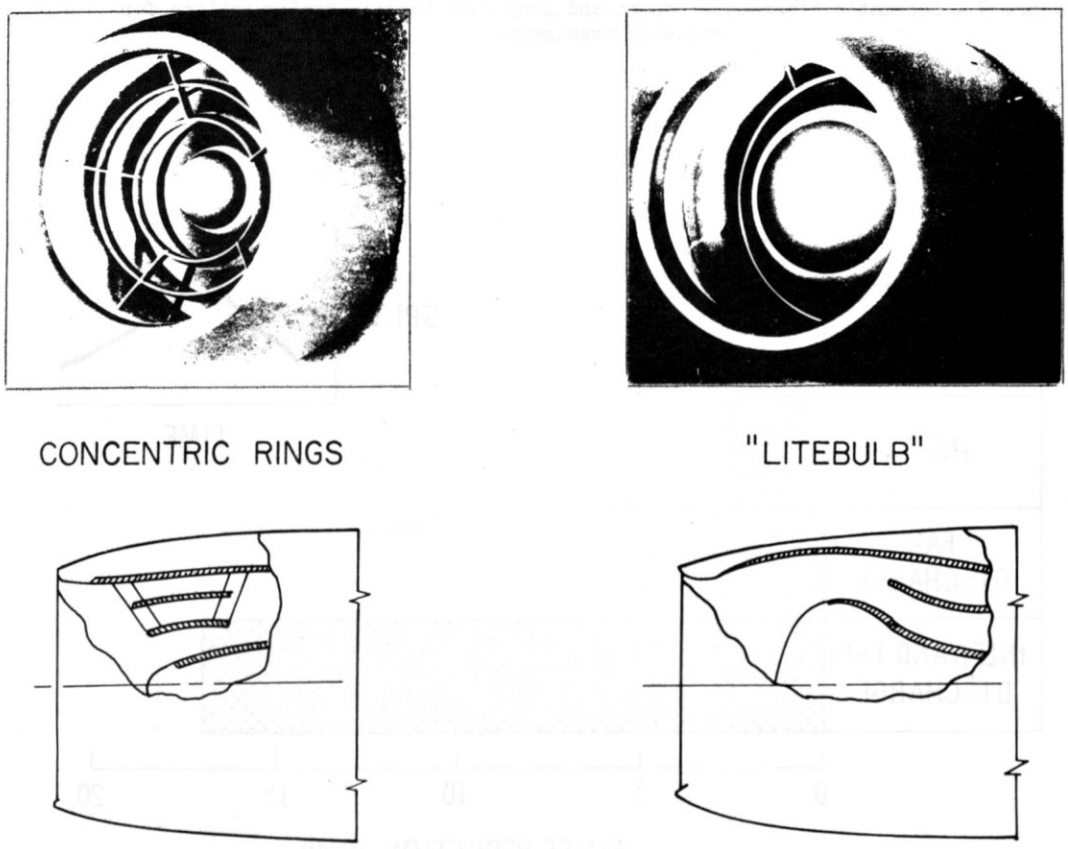

Figure 8.- Inlet configurations for acoustic treatment (ref. 12).

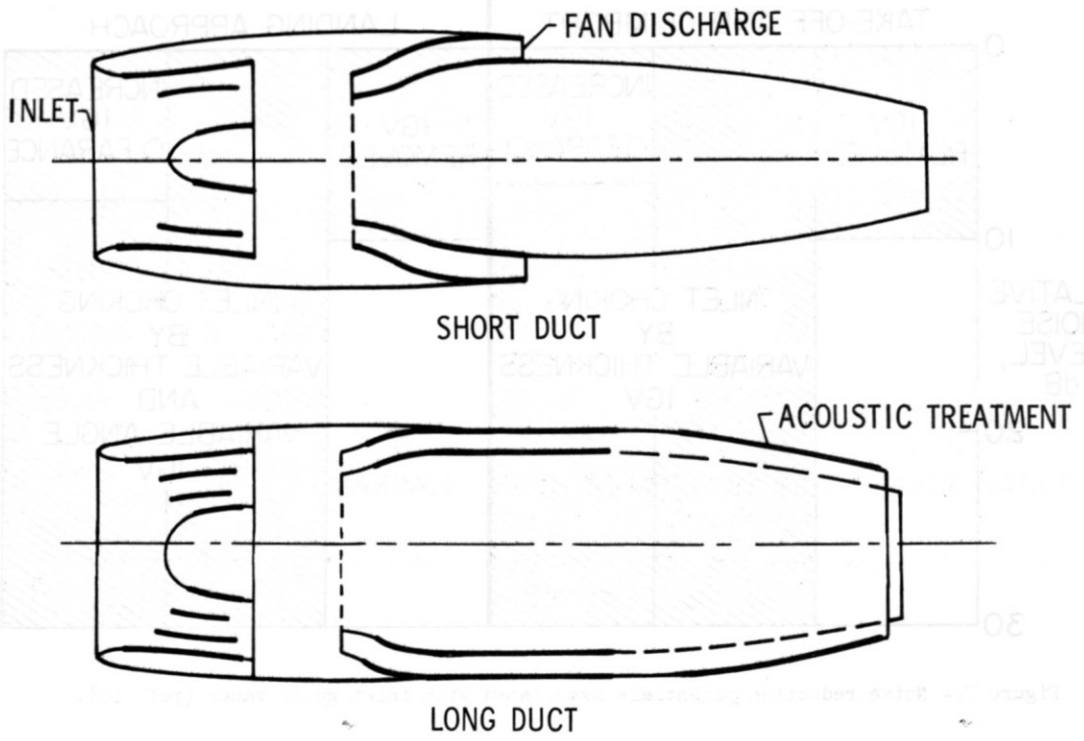

Figure 9.- Schematic diagrams of short and long duct nacelle configurations for acoustic treatment.

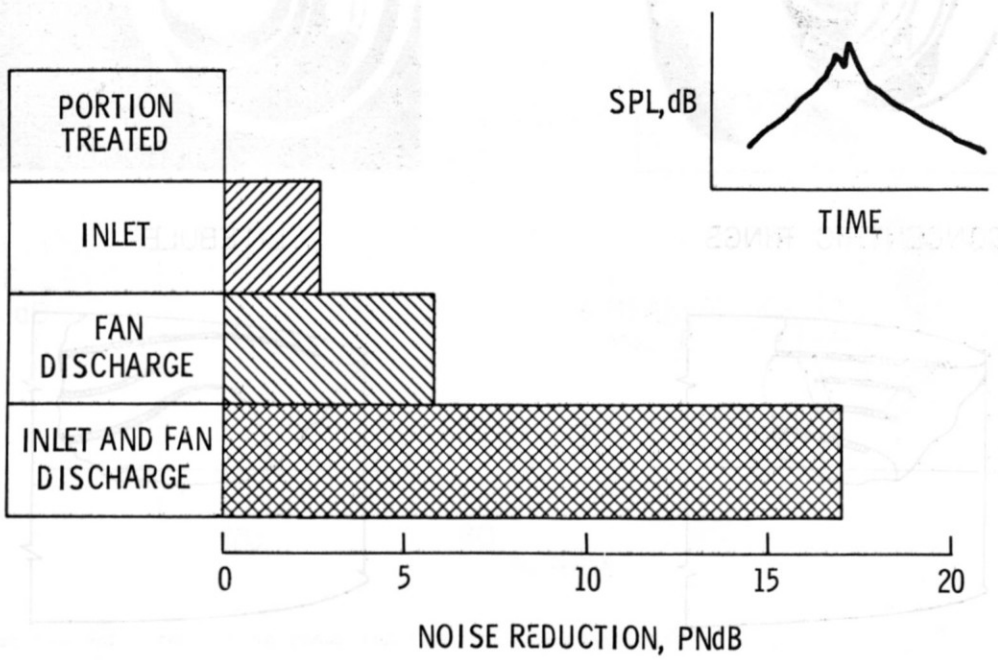

Figure 10.- Noise reduction potential of engine nacelle acoustic treatment (ref. 3).

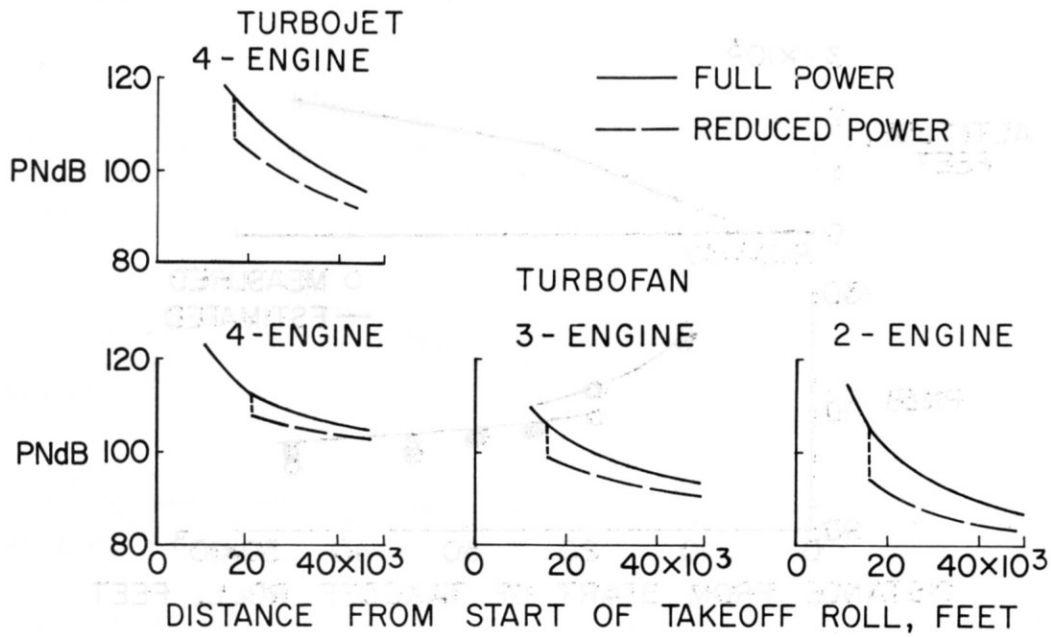

Figure 11.- Noise reduction resulting from power cutback for various type jet power plants (power reduced to that required for maintaining 500 fpm rate of climb) (ref. 13).

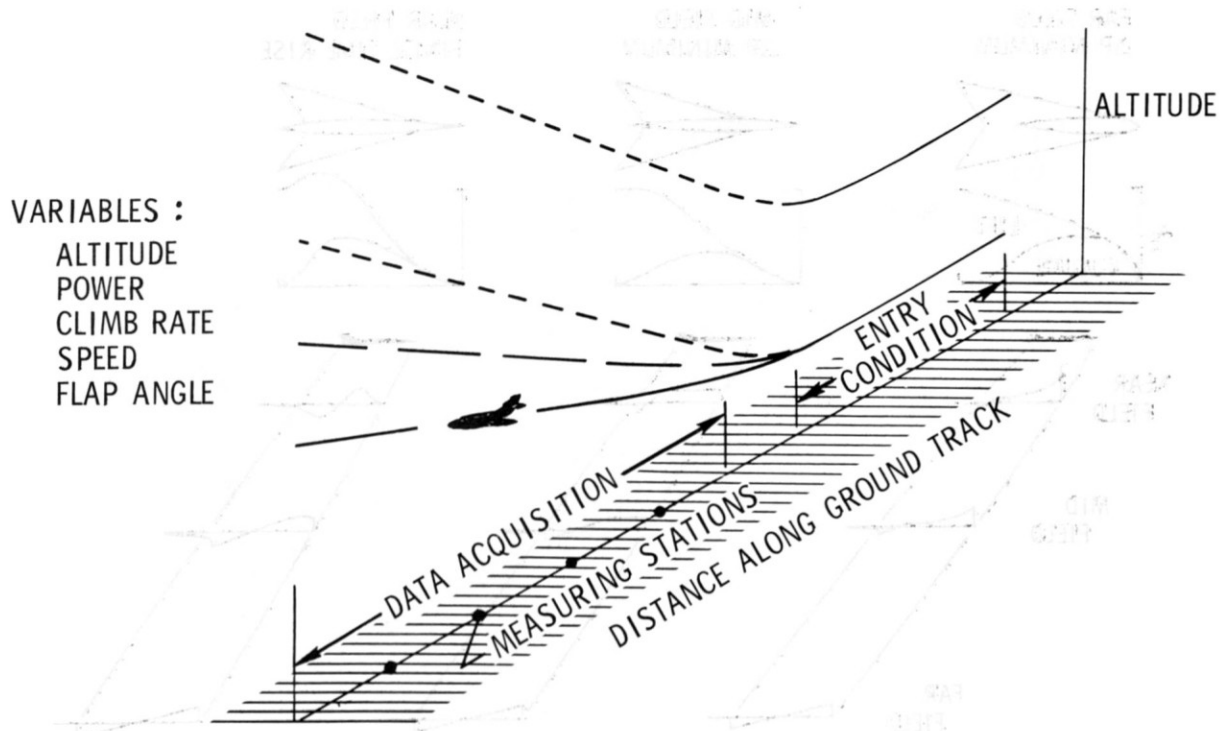

Figure 12.- Schematic diagram of test setup for simulating noise during take-off-climbout operations (ref. 13).

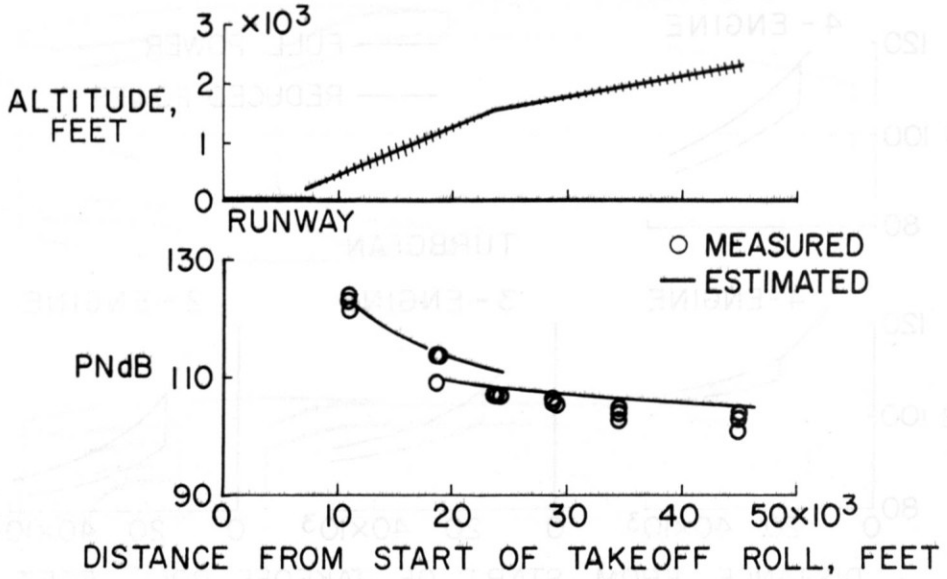

Figure 13.- Comparison of measured and estimated noise levels during climbout of four-engine turbojet powered aircraft (ref. 13).

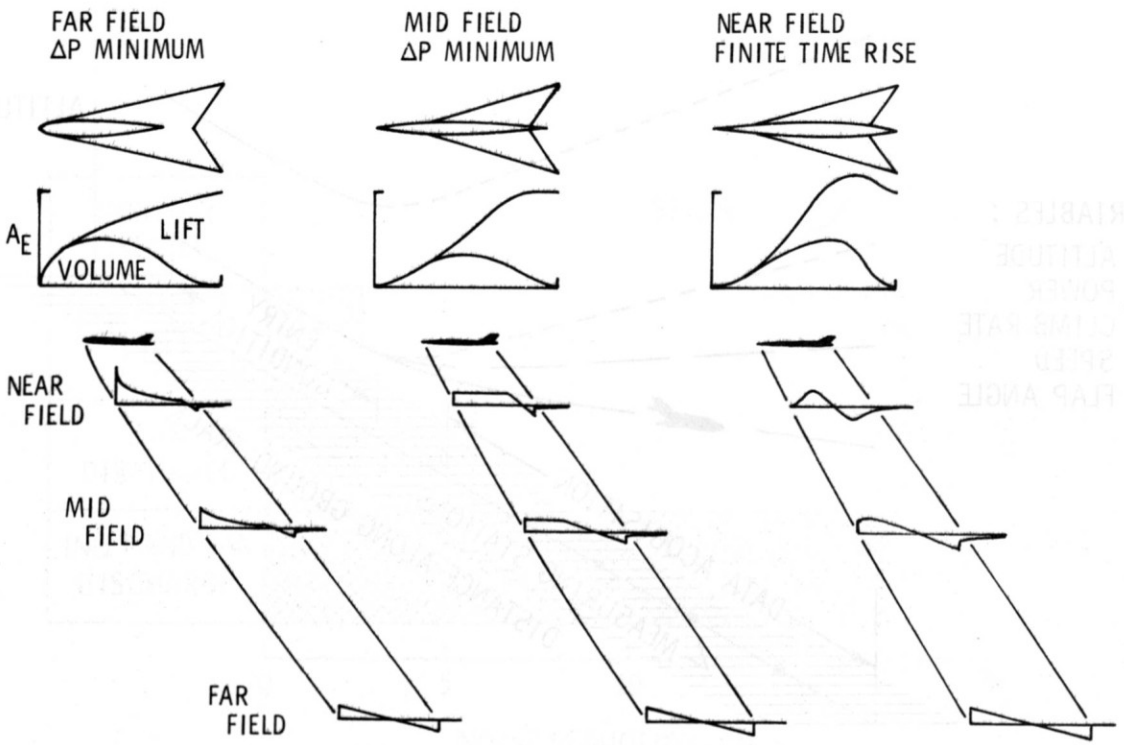

Figure 14.- Sonic boom minimization concepts (ref. 5).

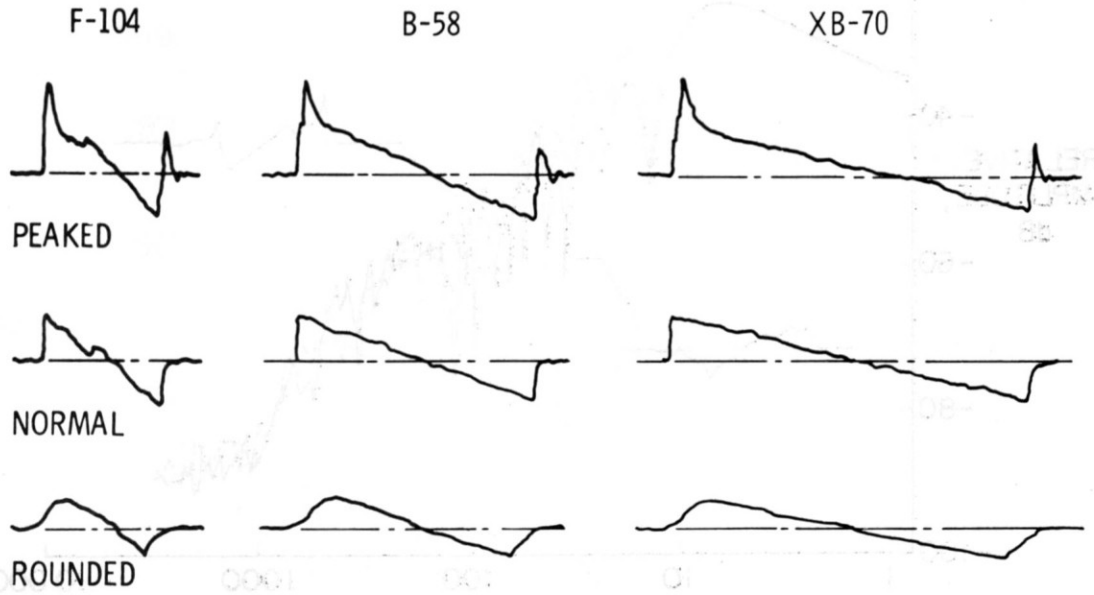

Figure 15.- Variation of measured sonic boom pressure signatures at ground level for small, medium, and large aircraft in steady-level flight (ref. 8).

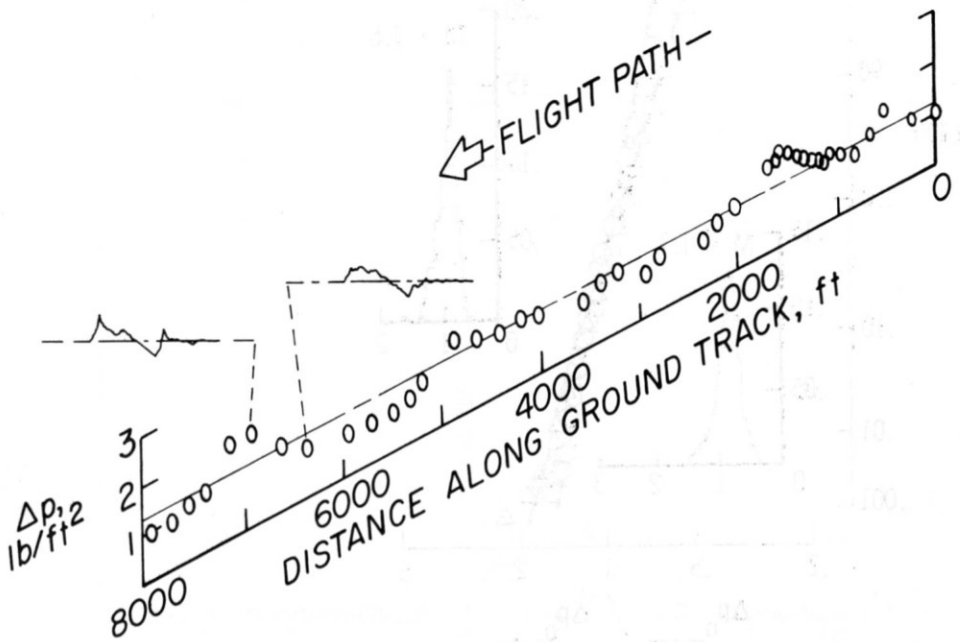

Figure 16.- Overpressure as a function of distance on the ground track for an F-104 airplane in steady flight at a Mach number of 1.3 and an altitude of 30,500 feet and sample signatures (ref. 8).

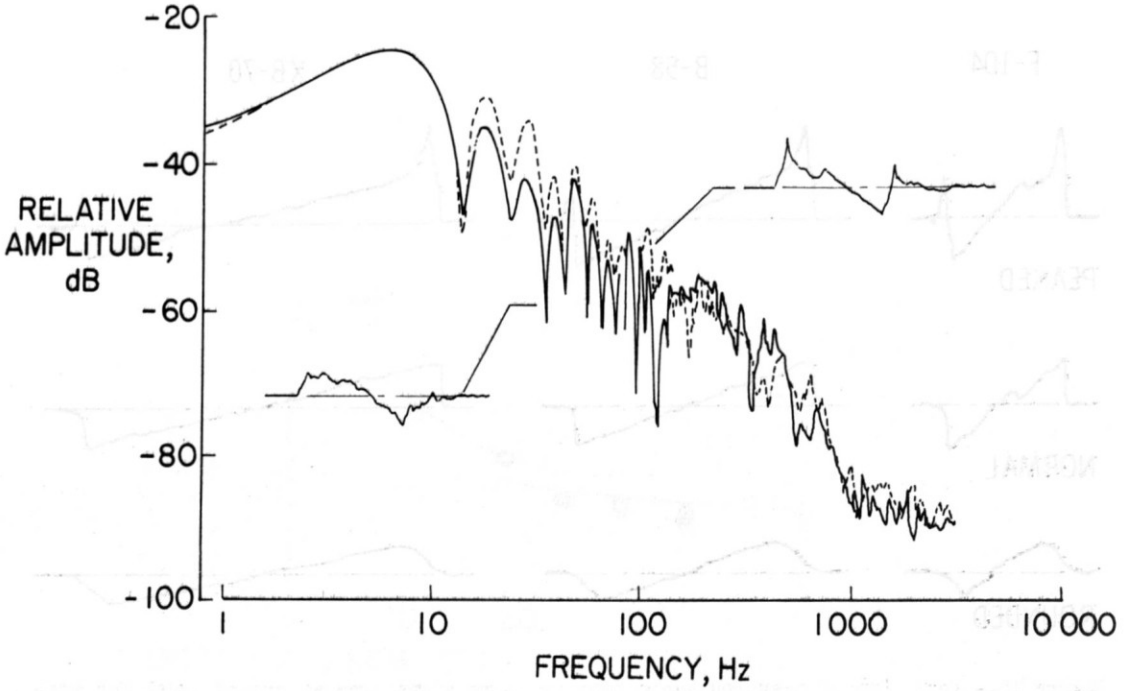

Figure 17.- Energy spectra for two different shapes of sonic-boom pressure signatures. Relative amplitude is given by $10 \log_{10} /f(\omega)/^2$ dB (ref. 8).

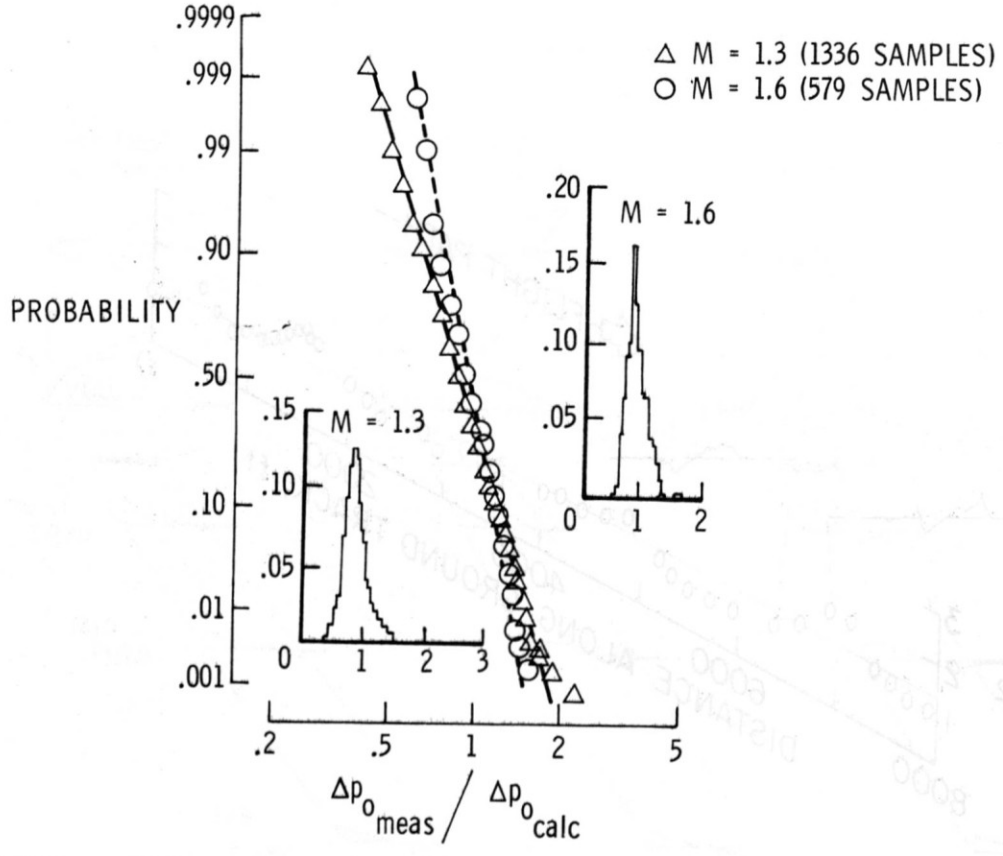

Figure 18.- Probability of exceeding a given value of the ratio of measured to calculated ground overpressures along the flight track of the F-104 airplane at an altitude of about 30 000 feet for two Mach numbers (ref. 14).

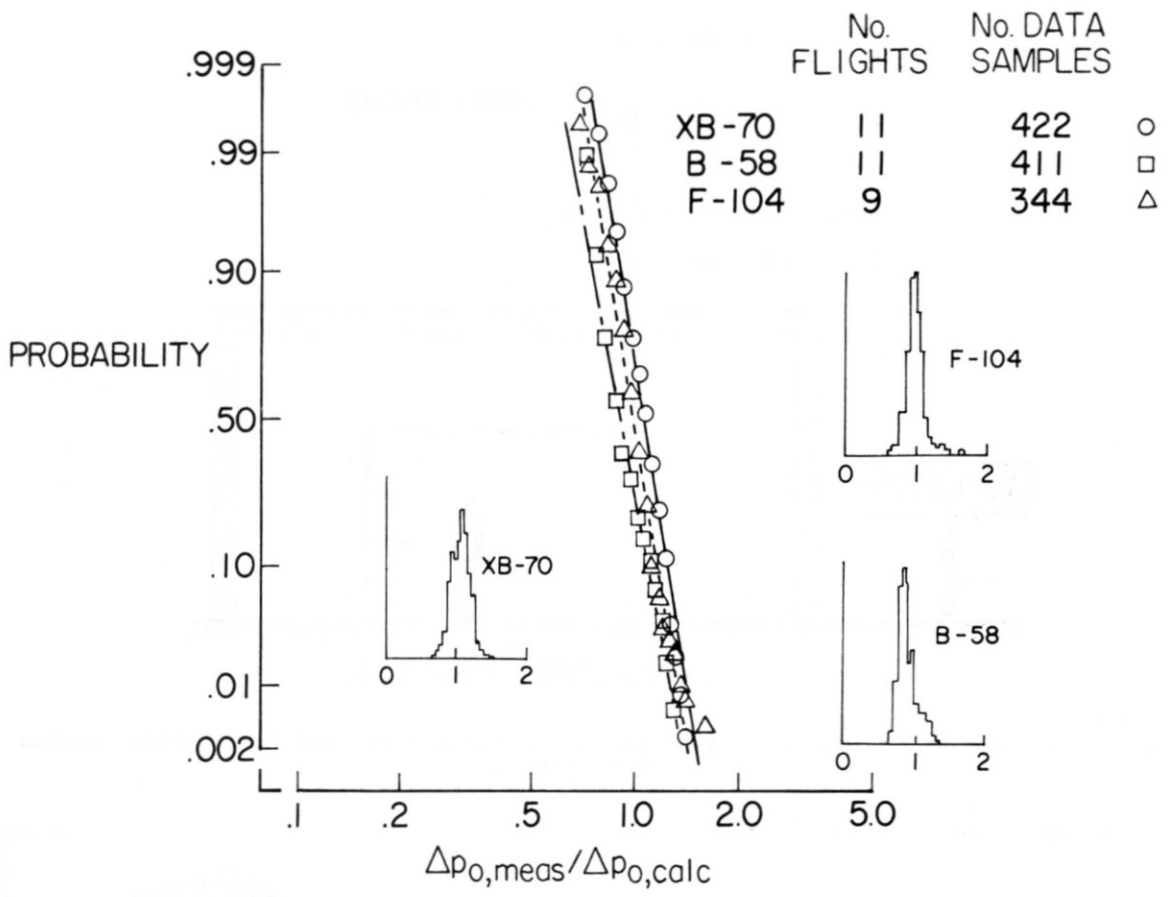

Figure 19.- Probability of exceeding a given value of the ratio of measured to calculated ground overpressures along flight track for XB-70, B-58, and F-104 airplanes. (Time intervals of flights of three airplanes varied from about 2 to 5 minutes) (ref. 8.)

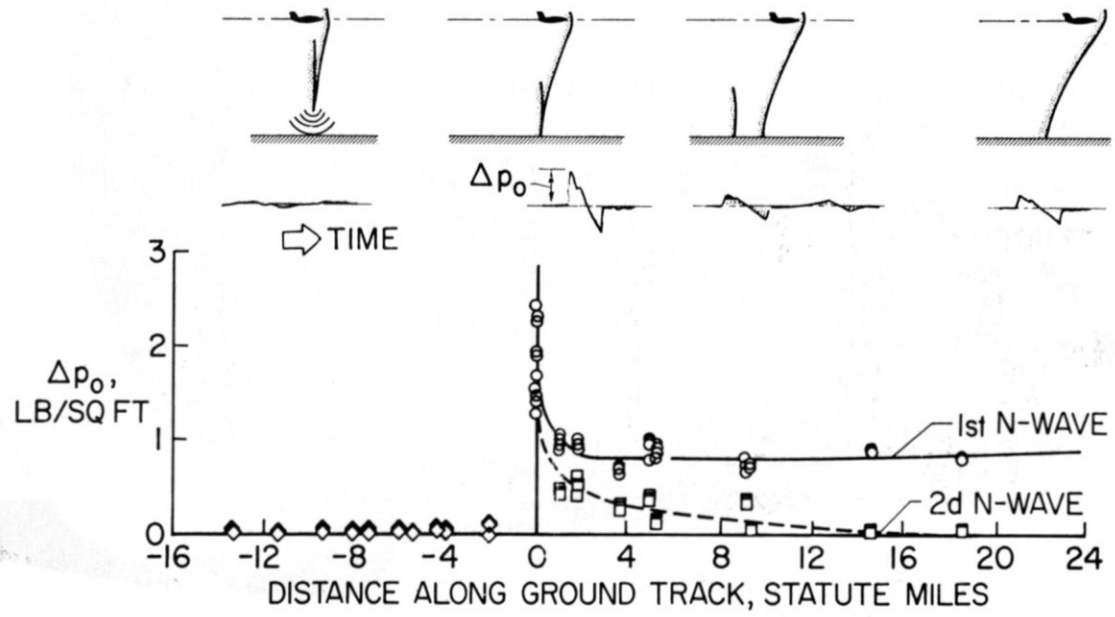

Figure 20.- Sonic boom overpressure measurements along the ground track for an aircraft in accelerated flight at constant altitude (ref. 15).

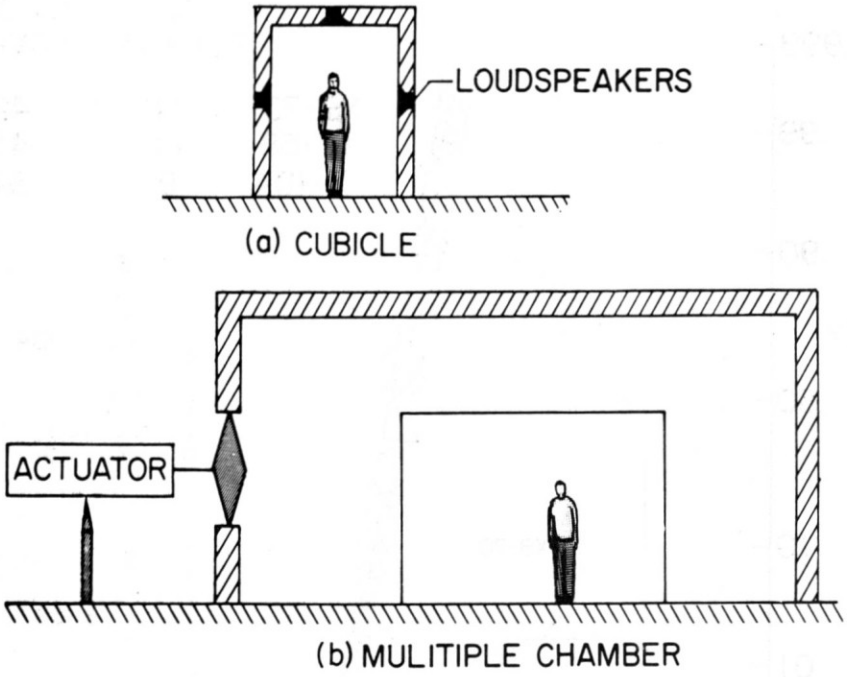

Figure 21.- Schematic diagrams of two types of sonic boom simulators used for subjective studies (refs. 16 and 17).

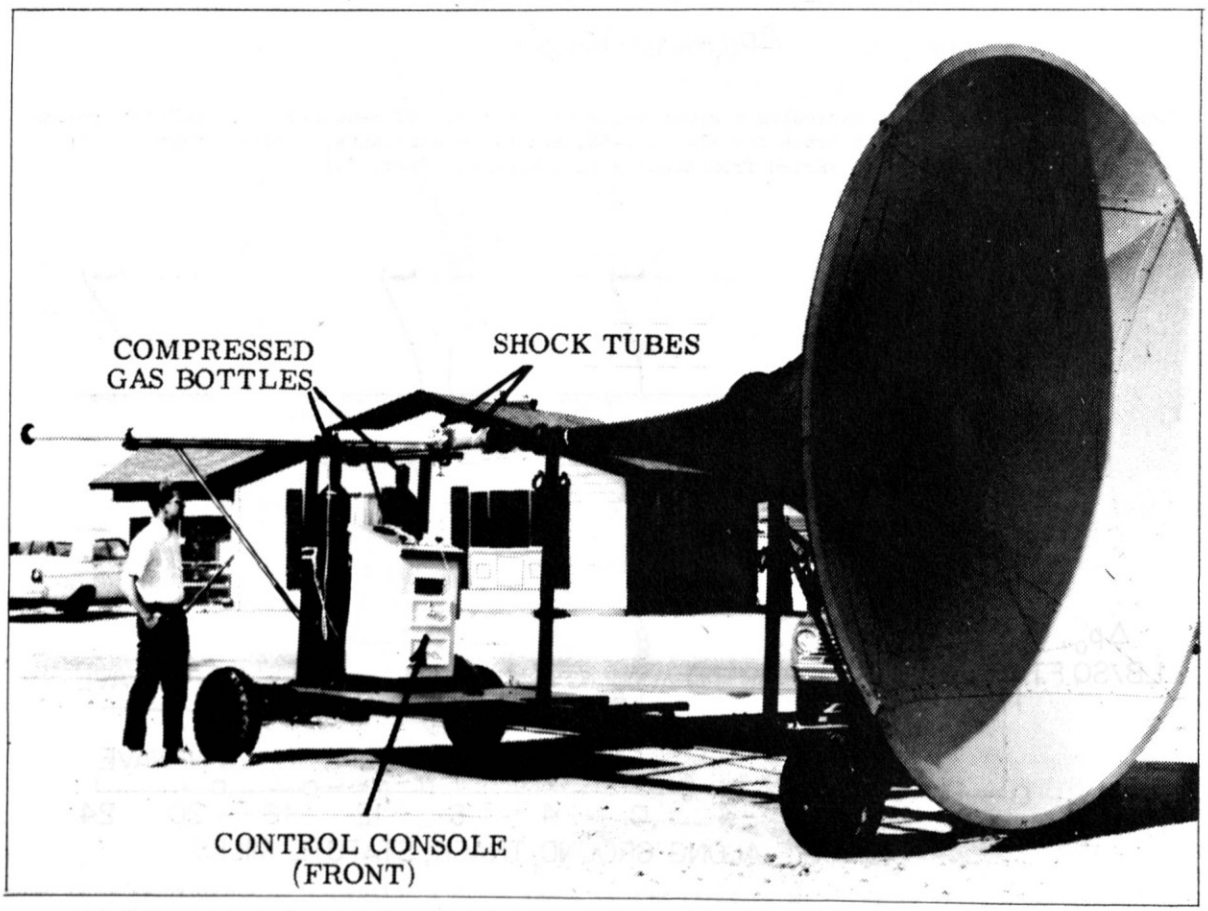

Figure 22.- Photograph of shock tube type sonic-boom simulator (ref. 18).

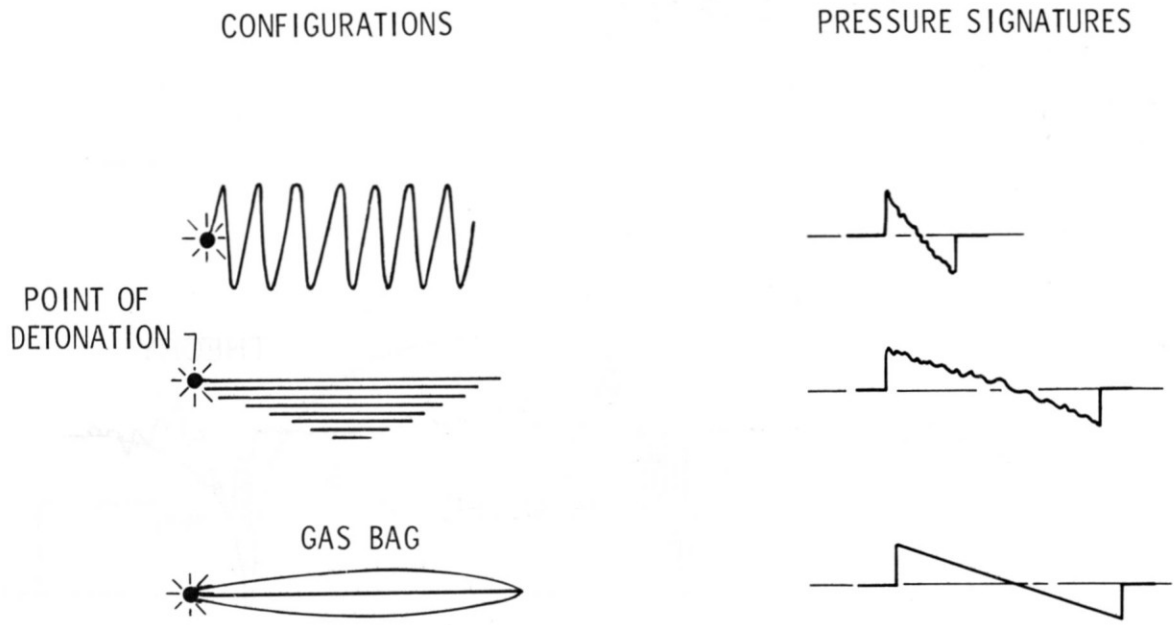

Figure 23.- Schematic diagrams of three explosive charge configurations for simulating sonic booms.

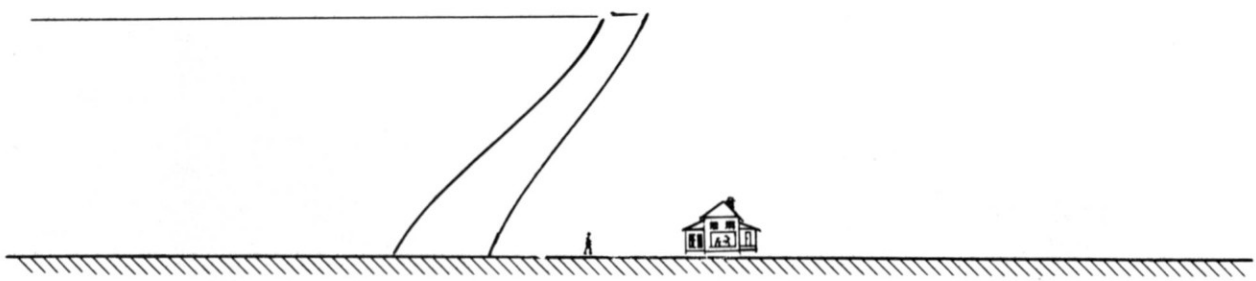

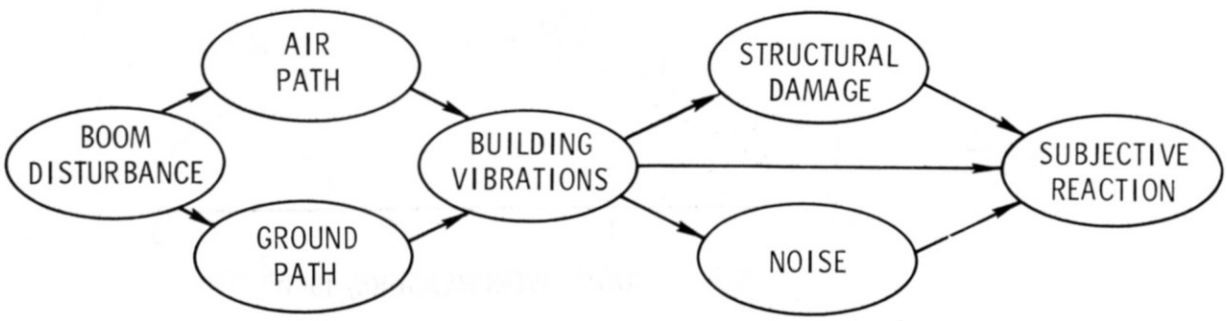

Figure 24.- Factors involved in sonic-boom exposures (ref. 5).

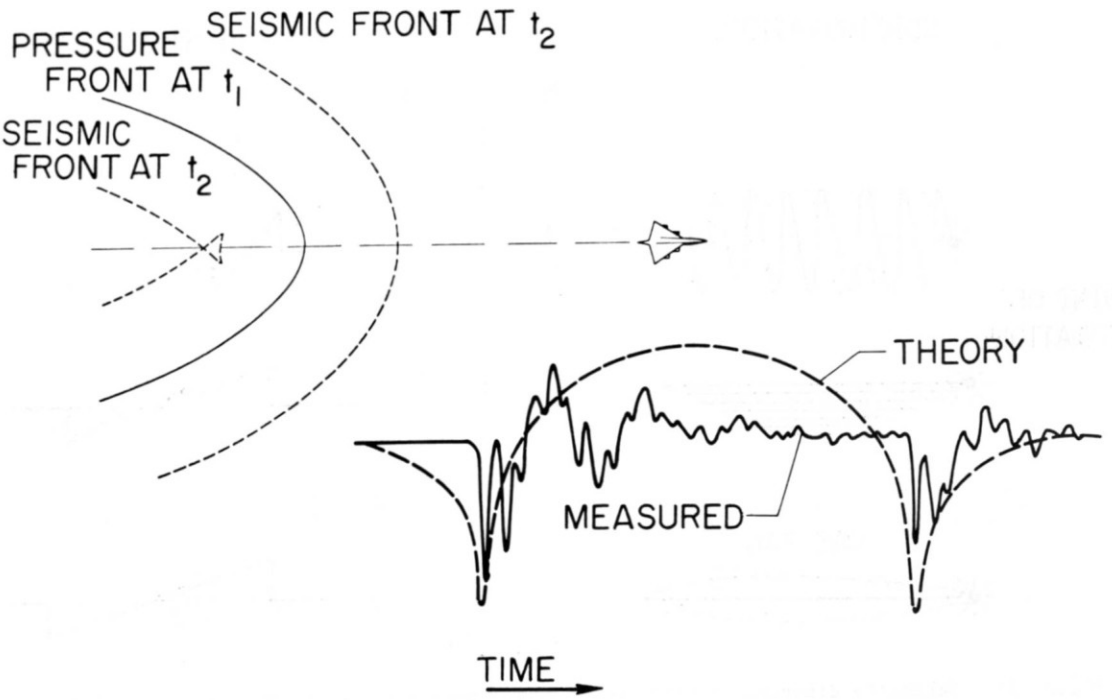

Figure 25.- Measured sonic boom induced ground particle velocity signature (ref. 19).

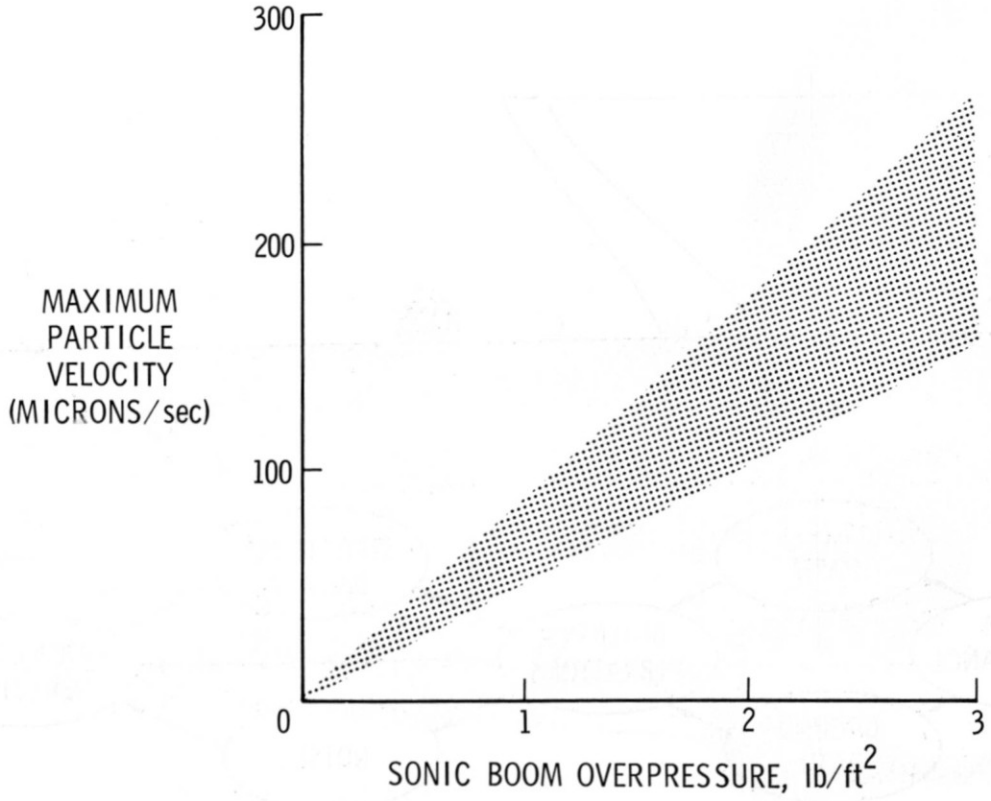

Figure 26.- Ground particle velocities as a function of sonic-boom overpressure (ref. 19).

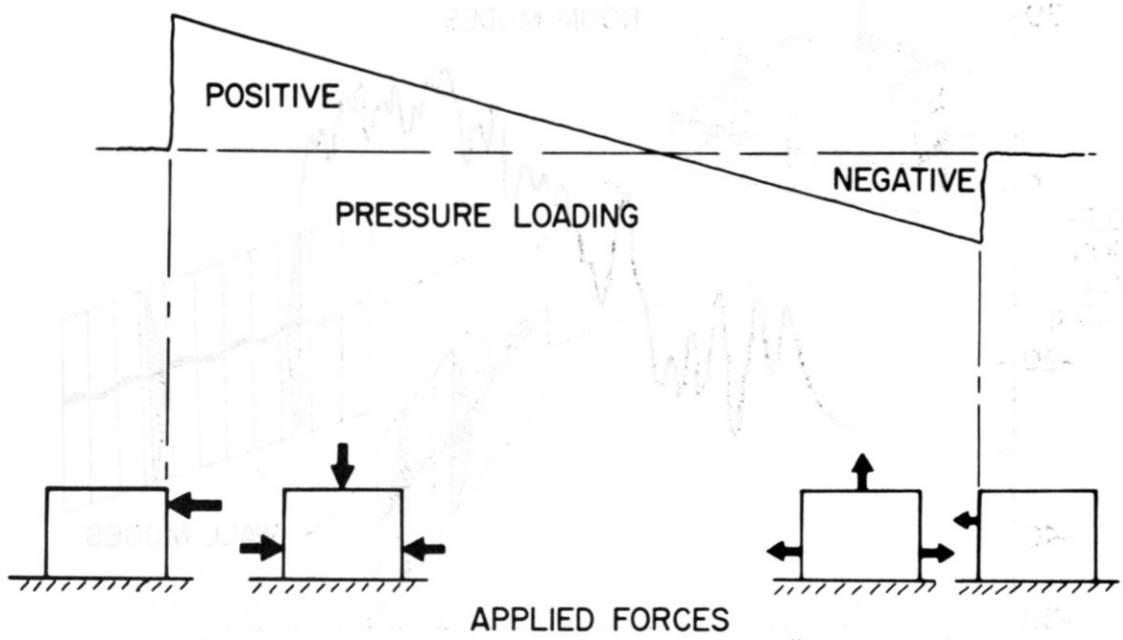

Figure 27.- Sonic-boom loading on buildings (ref. 5).

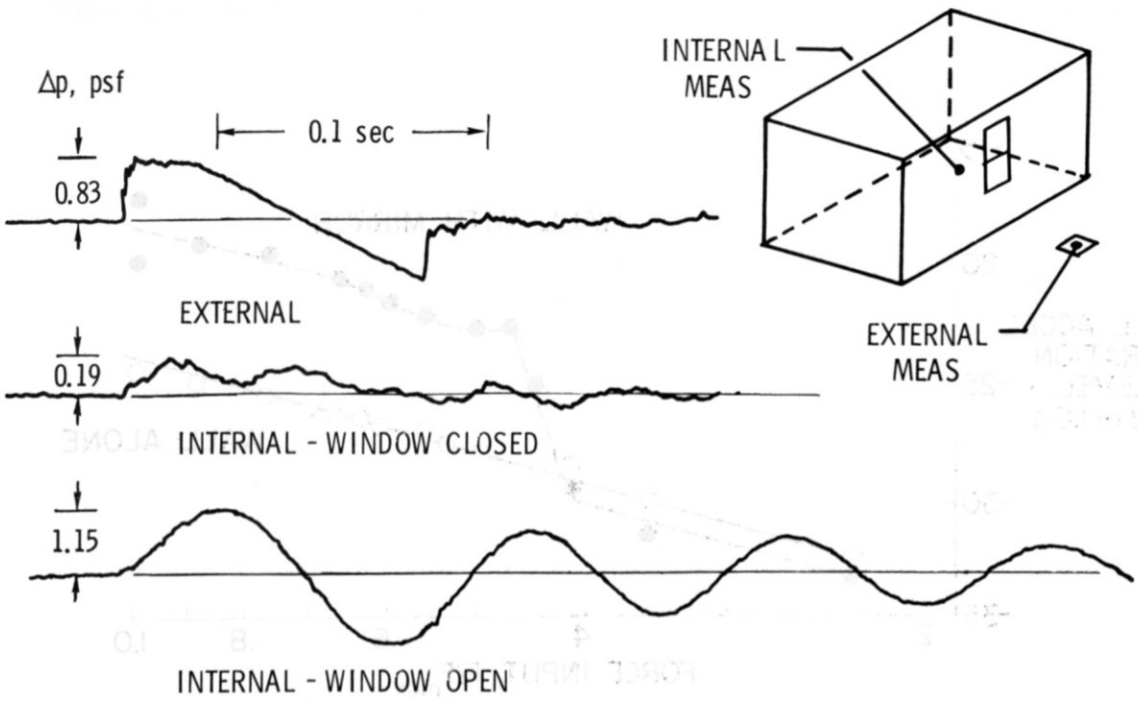

Figure 28.- Internal room pressure time histories due to sonic booms for both window-closed and window-opened conditions (ref. 5).

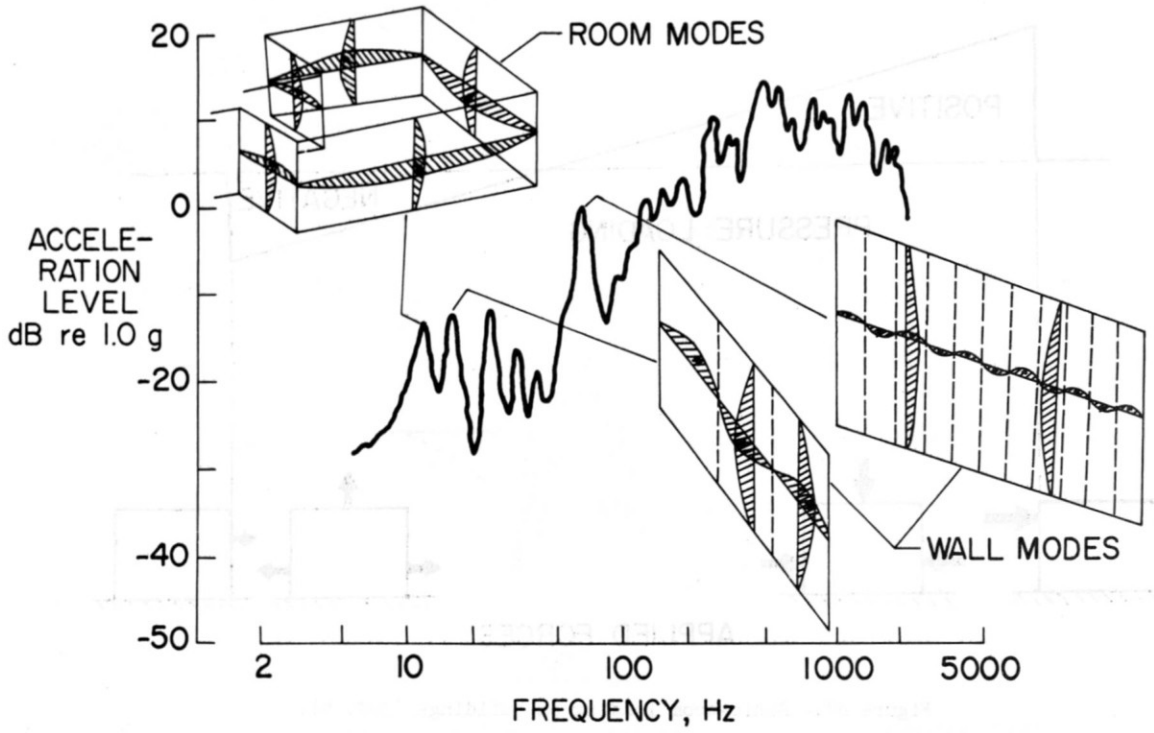

Figure 29.- House acceleration level as a function of frequency for a constant exciting force

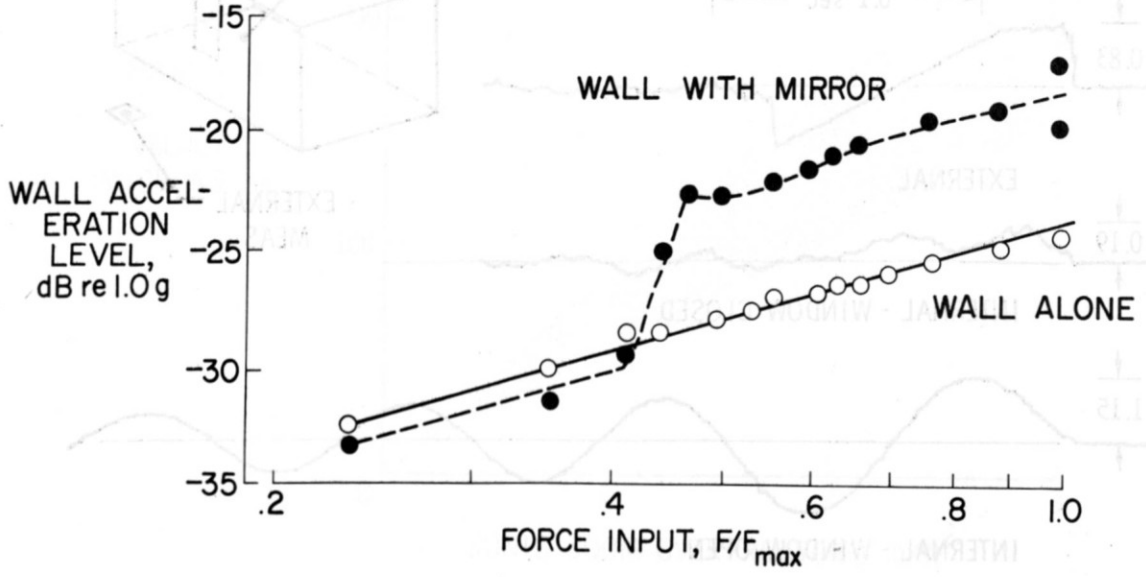

Figure 30.- Acceleration levels as a function of force input for a wall with and without a hanging mirror

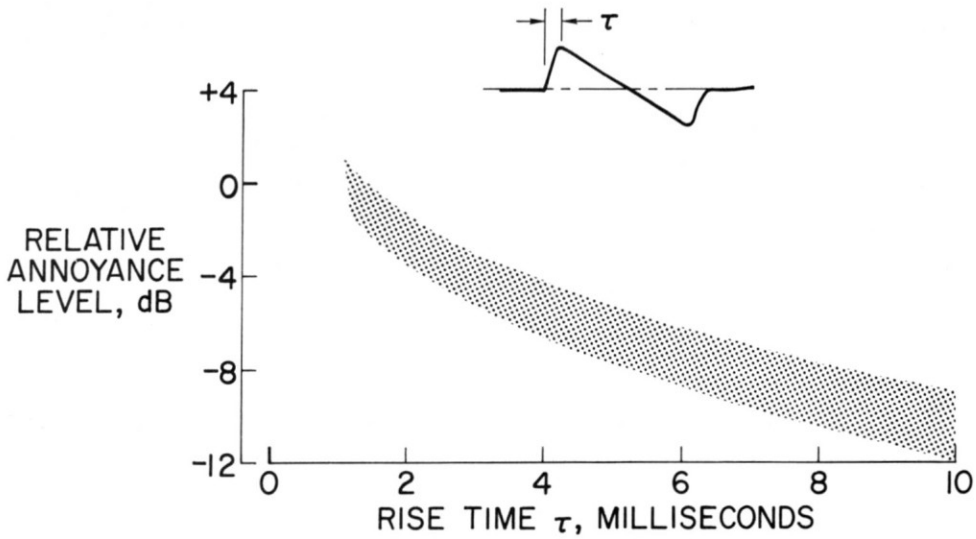

Figure 31.- Effects of rise time on the relative annoyance levels of sonic booms (ref. 16).